Structure in Radiative Shock Experiments

Forrest Doss

SSGF Annual Meeting
6/21/2010

This work is funded by the DOE NNSA-DS and SC-OFES Joint Program in High-Energy-Density Laboratory Plasmas by grant DE-FG52-09NA29548, by the National Laser User Facility Program in NNSA-DS by grant DE-FG52-09NA29034, by the Predictive Sciences Academic Alliances Program in NNSA-ASC by grant DE-FC52-08NA28616, and by the DOE Stewardship Science Graduate Fellowship program.

We call shock waves radiative when…

- Radiative energy flux would exceed incoming material energy flux

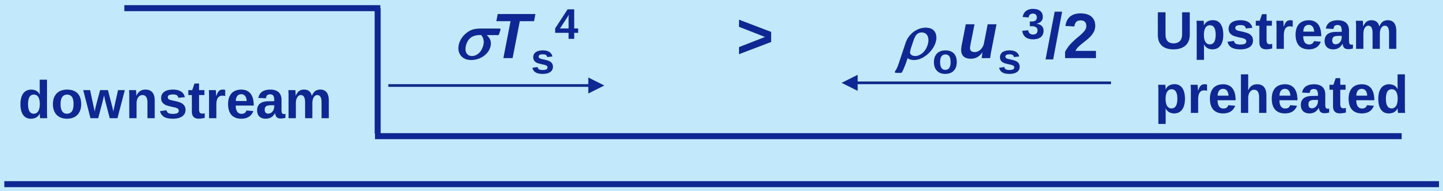

downstream

$\sigma T_s^4 \quad > \quad \rho_o u_s^3/2$

Upstream preheated

where post-shock temperature is proportional to u_s^2 in simple shock model.

- The ratio of these energy fluxes is proportional to u_s^5/ρ_o, so for high enough u_s, radiation dominates.

This research was supported by the DOE NNSA/ASC under the Predictive Science Academic Alliance Program by grant number DEFC52-08NA28616.

Conservation of energy forces the shock wave to develop complex structure

Shocked xenon layer
Compressed > 20x

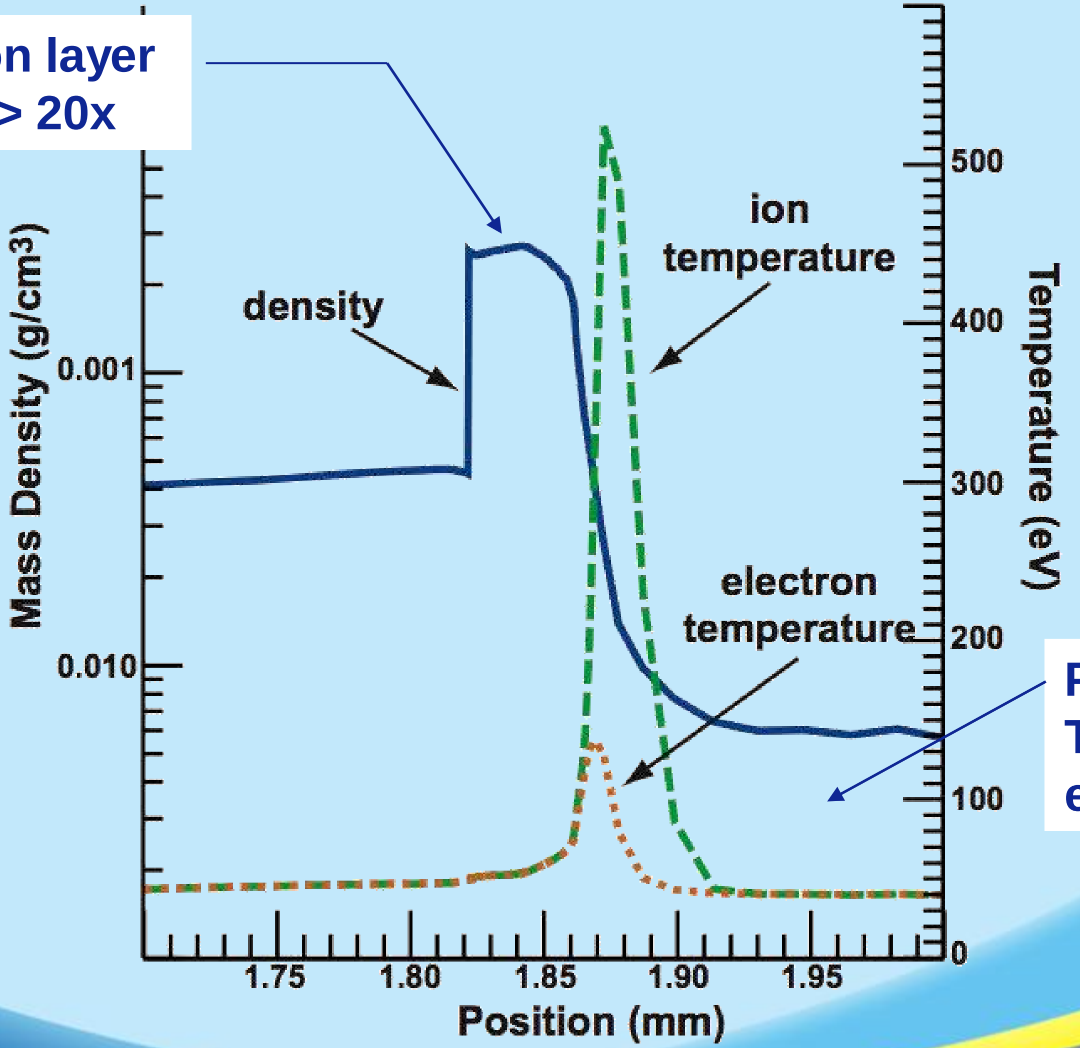

Preheated region
Thermal photons escape upstream

This research was supported by the DOE NNSA/ASC under the Predictive Science Academic Alliance Program by grant number DEFC52-08NA28616.

Shocks in supernovae pass through the regime of our experiments as they emerge

Ensman and Burrows, *ApJ.*, 393,742-755,1992

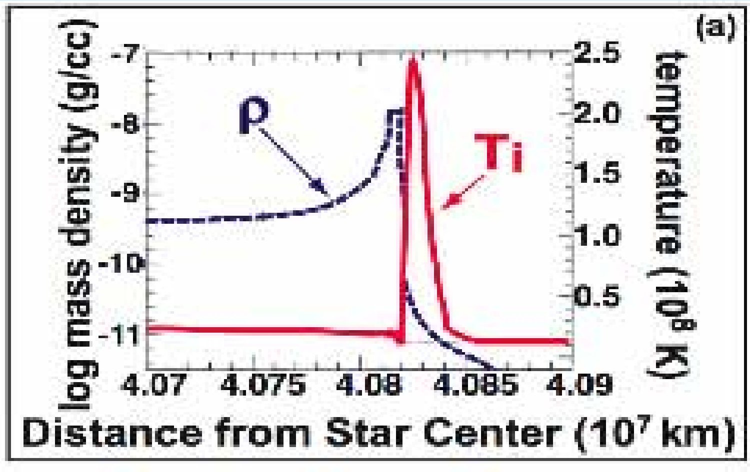

1987A simulation

A.B. Reighard (Cooper), POP, 2007

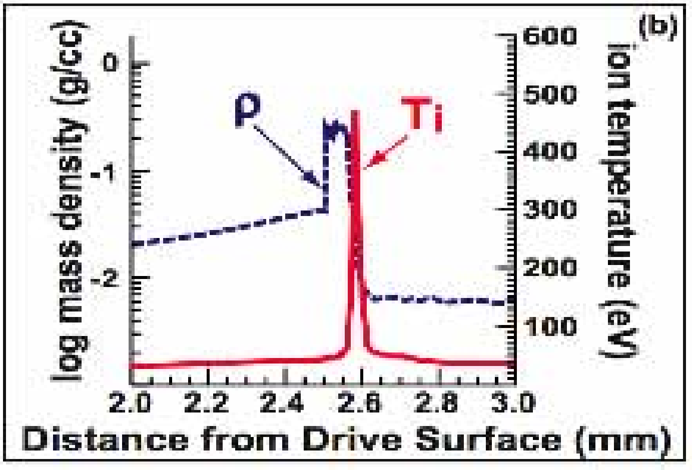

Xe experiment simulation

- Core collapse SN shock develops a thin dense shell.
  - This occurs once radiation ahead of the shock can escape.
  - This should lead to increase in luminosity.
  - Breakup of dense shell is of interest and will impact later SNR structure.

This research was supported by the DOE NNSA/ASC under the Predictive Science Academic Alliance Program by grant number DEFC52-08NA28616.

Experiments are conducted in directly driven xenon-filled shock tubes on the Omega laser

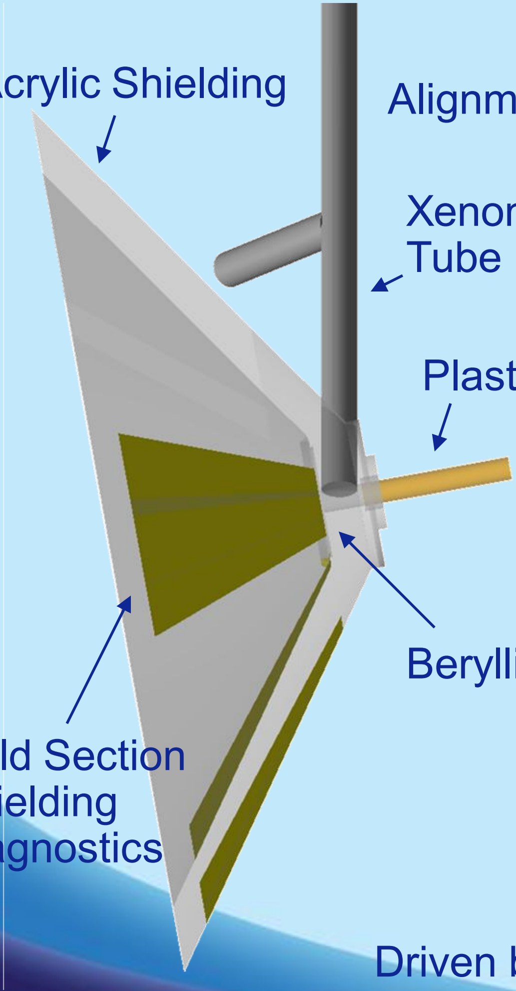

Acrylic Shielding

Alignment Fiducial

Xenon Gas Fill Tube / Stalk

Plastic Shock Tube

Beryllium Drive Disc

Gold Section Shielding Diagnostics

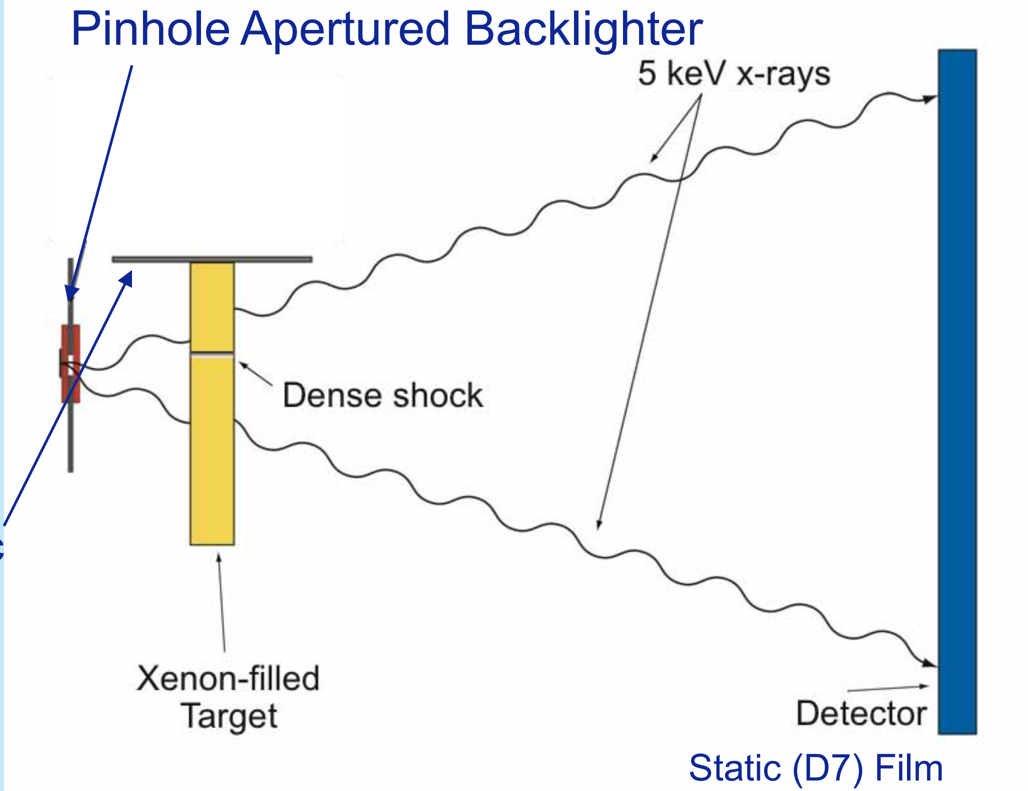

Pinhole Apertured Backlighter

Static (D7) Film

Driven by 1 ns, 4 kJ, square pulse

This research was supported by the DOE NNSA/ASC under the Predictive Science Academic Alliance Program by grant number DEFC52-08NA28616.

Radiography measures shock features

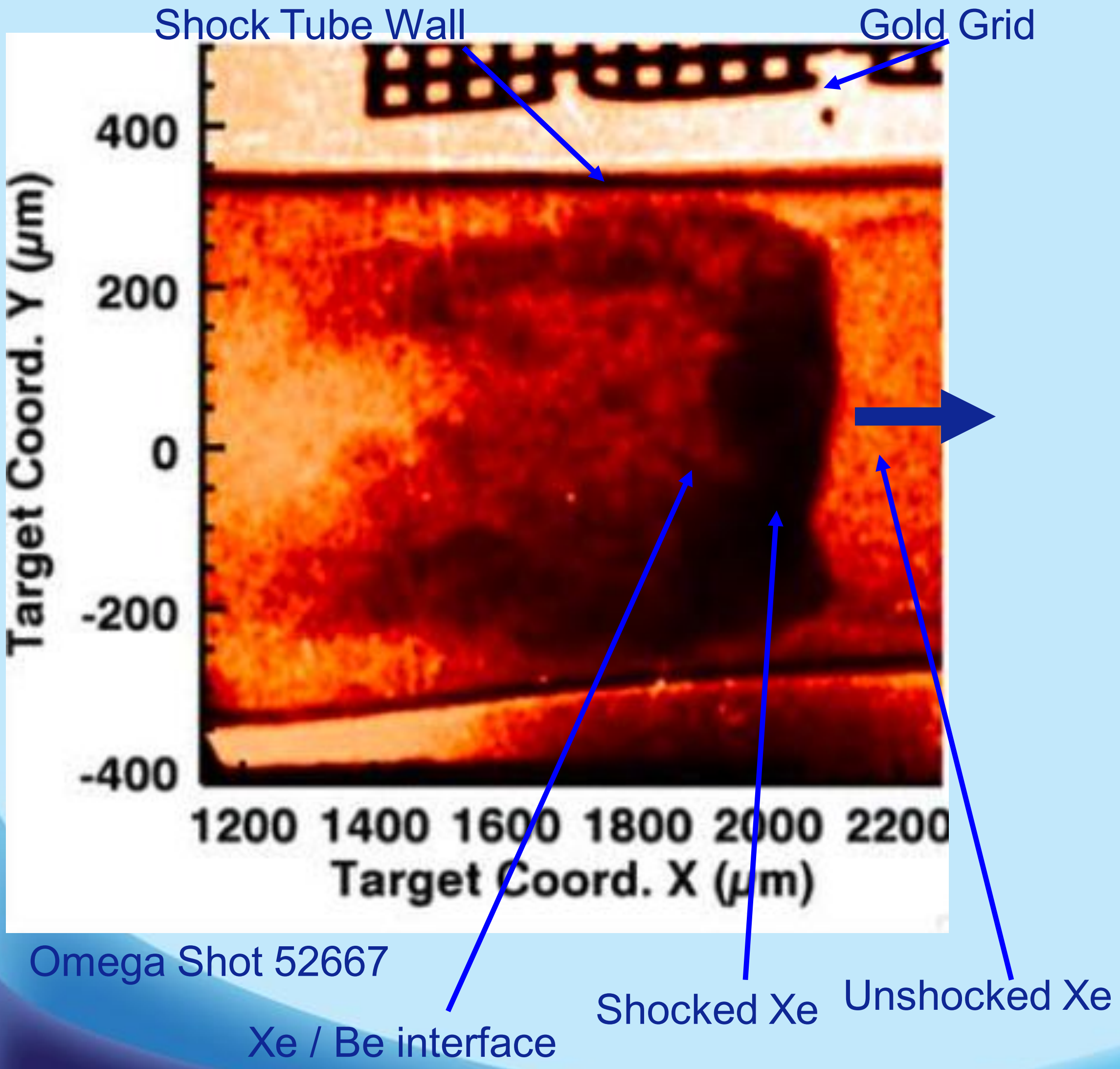

- Shock is driven by 20 µm Be disc, t = 13 ns, shock traveling at ~110 km/sec.
- Shock has traveled 2 mm, apparently compressed material to < 150 µm.
- Gold Grid serves as a spatial fiducial. Data from pre-shot metrology is used to diagnose lengths in target image.
- No transmission through the dense layer.

This research was supported by the DOE NNSA/ASC under the Predictive Science Academic Alliance Program by grant number DEFC52-08NA28616.

Repeatability Experiment:

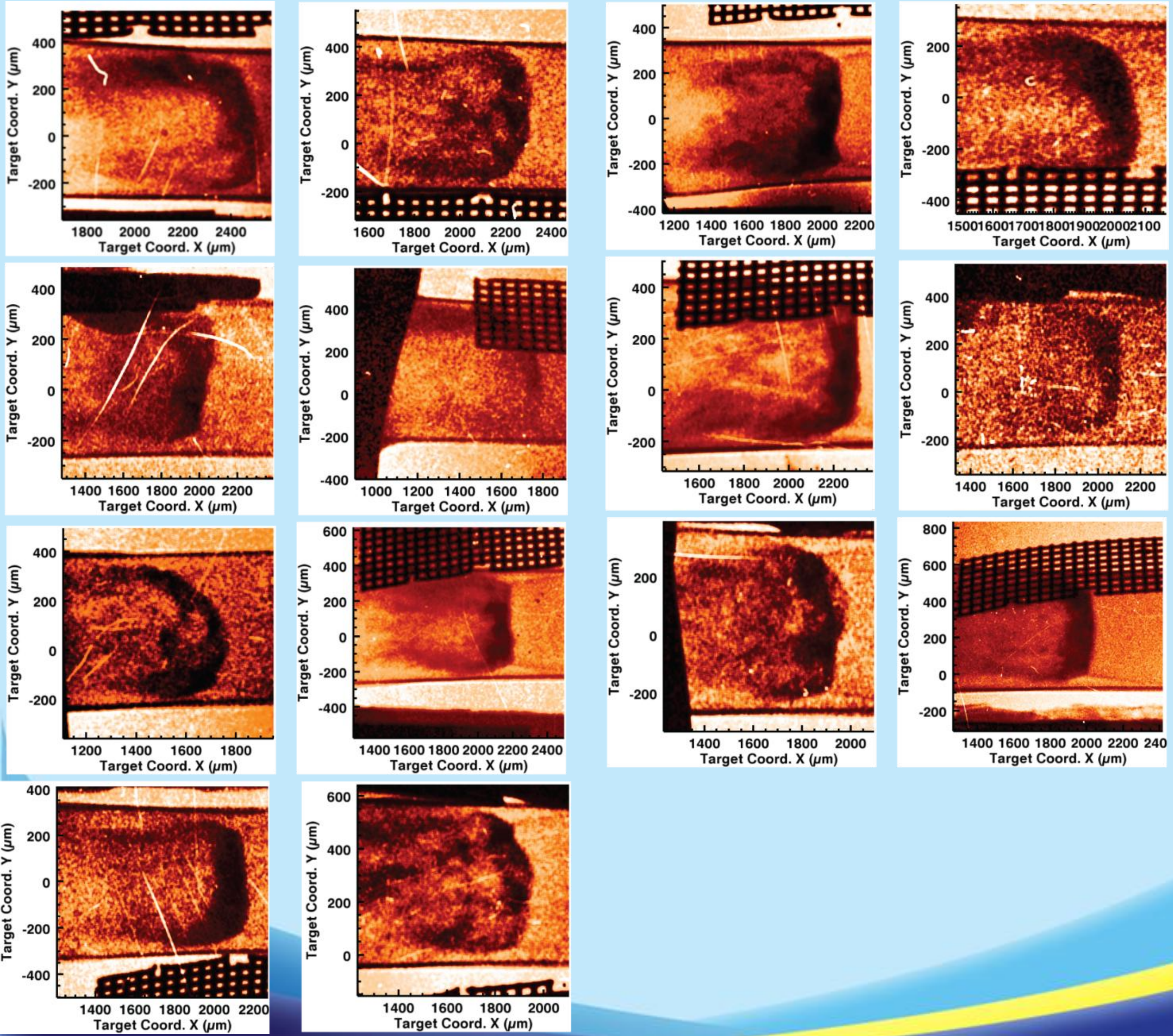

October 2008, we shot a campaign of nominally identical targets.

Achieved ~ 5% build variation, lower laser and gas variation, additional alignment variation on some shots, one known out-of-spec target.

This research was supported by the DOE NNSA/ASC under the Predictive Science Academic Alliance Program by grant number DEFC52-08NA28616.

We infer mean shock compression

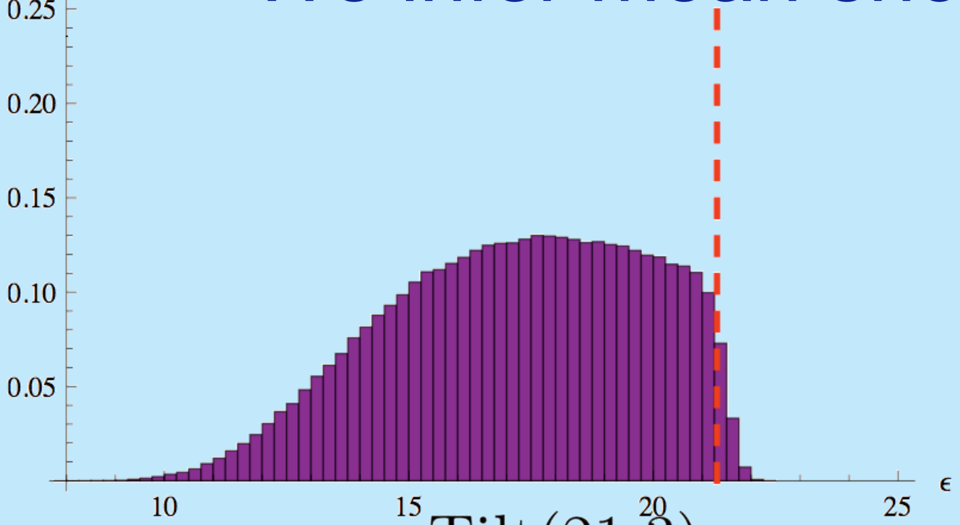

$\epsilon \sim \mathrm{Tilt}(21.3)$

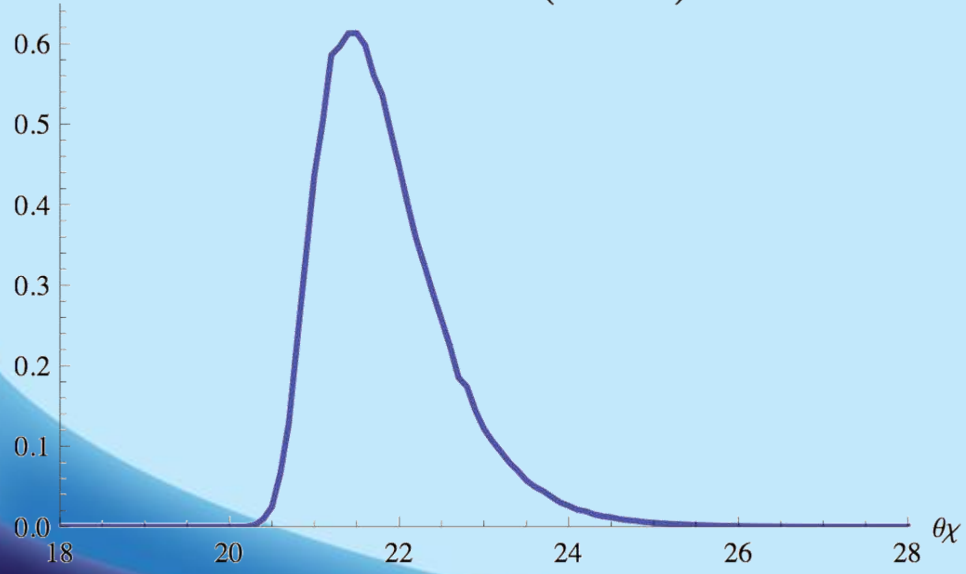

P(θχ|data)

- For a given true mean compression θχ, we generate a histogram of predicted observations.

- Observations are skewed to lower values.

- Fitting observed quantities to Tilt() distributions, we generate a distribution for θχ.

- Mode at 21.5, 95% interval asymmetrically distributed between [20.7,23.7].

- Probability 99.99% θχ > 20.2

This research was supported by the DOE NNSA/ASC under the Predictive Science Academic Alliance Program by grant number DEFC52-08NA28616.

Wall shocks control the lateral boundaries

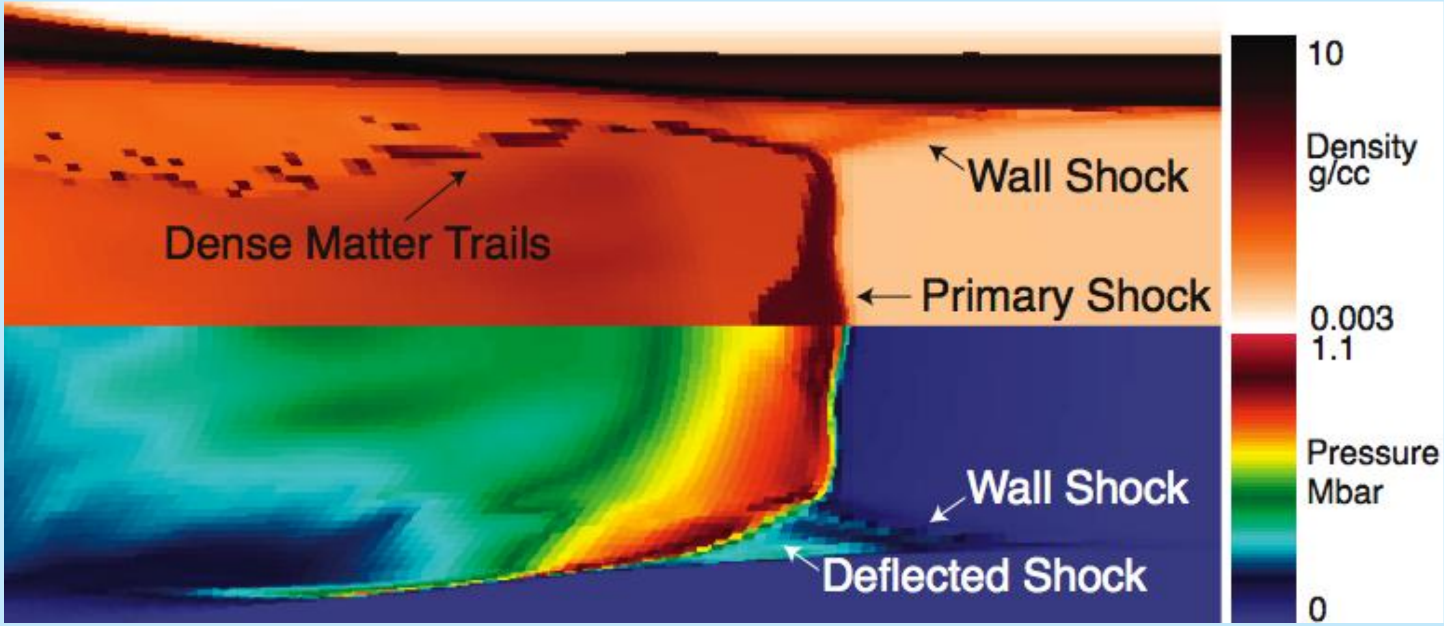

Doss, *Phys. Plasmas*,16(11):1 12705

High resolution HYDRA* simulation

- The shock tube is typically much denser and stronger than the interior material. Normally, the shock tube's evolution has small effects on material ahead of the shock.
- This assumption breaks down in HED systems.
- Radiation from the shock induces plastic ablation, forming a radial blast wave in the tube.

* M. M. Marinak et al., *Phys. Plasmas* 8, 2275 (2001)

This research was supported by the DOE NNSA/ASC under the Predictive Science Academic Alliance Program by grant number DEFC52-08NA28616.

Effects of the wall shock are clearly seen in radiating shock experiments

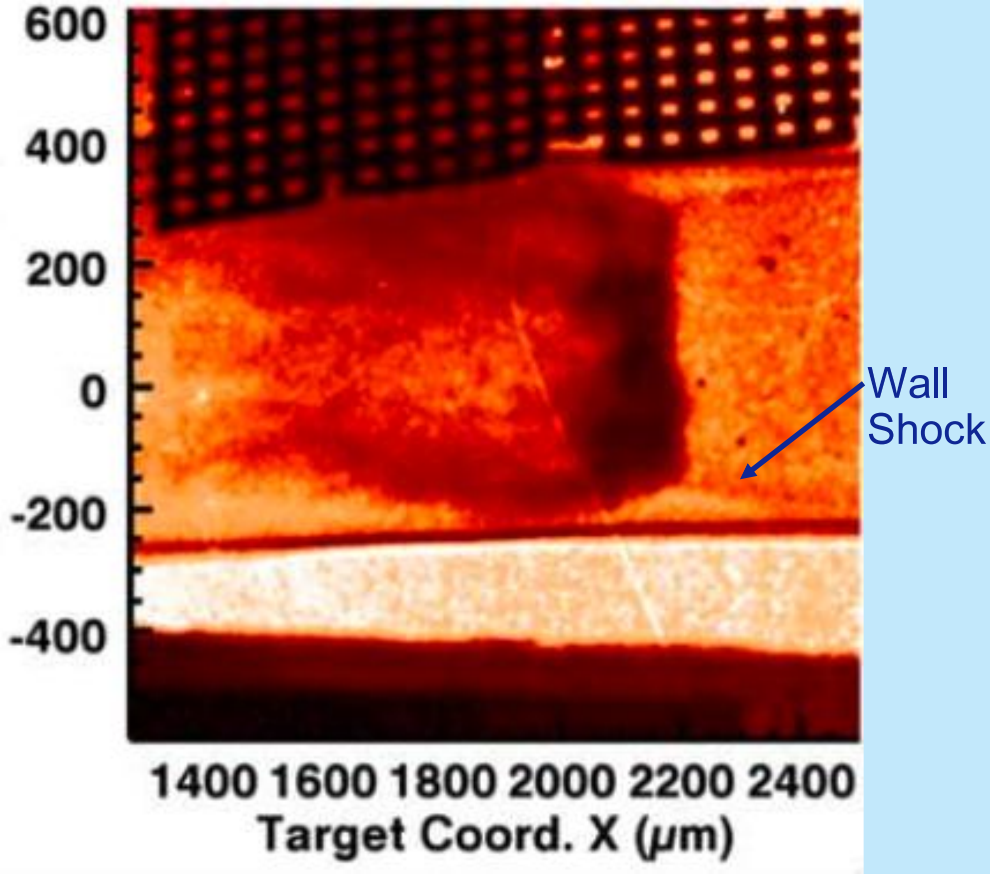

Omega Shot 52665

Wall shock induced features include:

- Finite displacement of shock edges from tube walls
- Angle of primary shock deflection at kink
- Angle of wall shock off of wall
- Curvature and thicknesses of the trails
- Dense Xenon collected behind the primary shock.

Wall shock features contain information.

This research was supported by the DOE NNSA/ASC under the Predictive Science Academic Alliance Program by grant number DEFC52-08NA28616.

The entrained flow behind the shock is also a consequence of the wall shocks

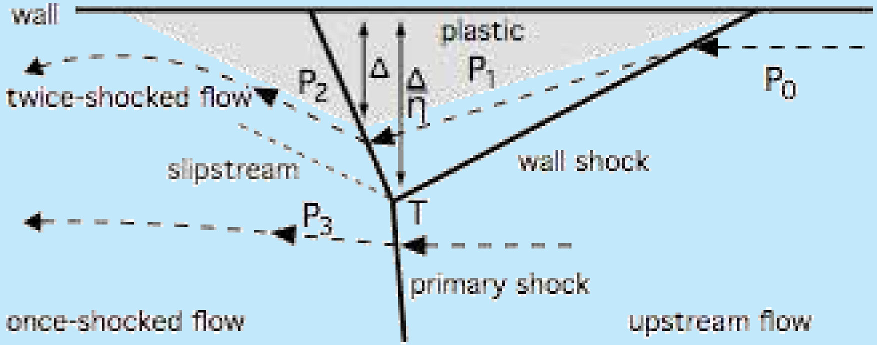

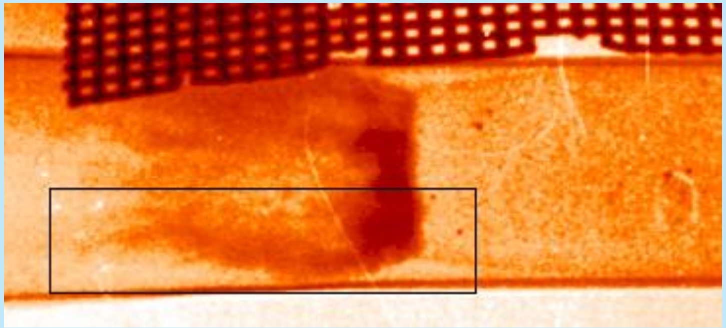

- Xenon which passes through multiple oblique shocks will exit the system faster than flow through a single normal shock.

- Mass swept up by wall shock around edge of the tube becomes the dense xenon in the entrained flow.

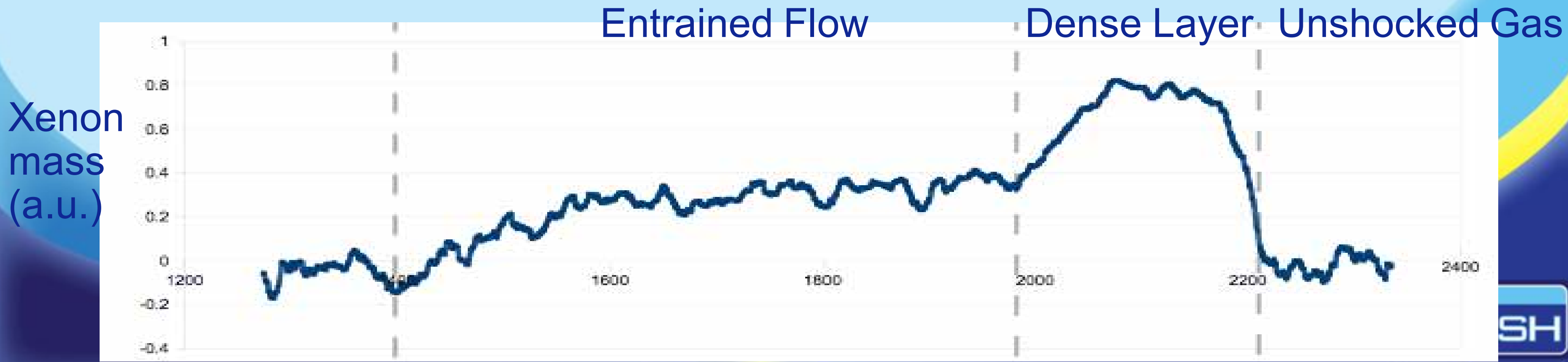

This research was supported by the DOE NNSA/ASC under the Predictive Science Academic Alliance Program by grant number DEFC52-08NA28616.

Results of analysis show structure internal to shocked layer

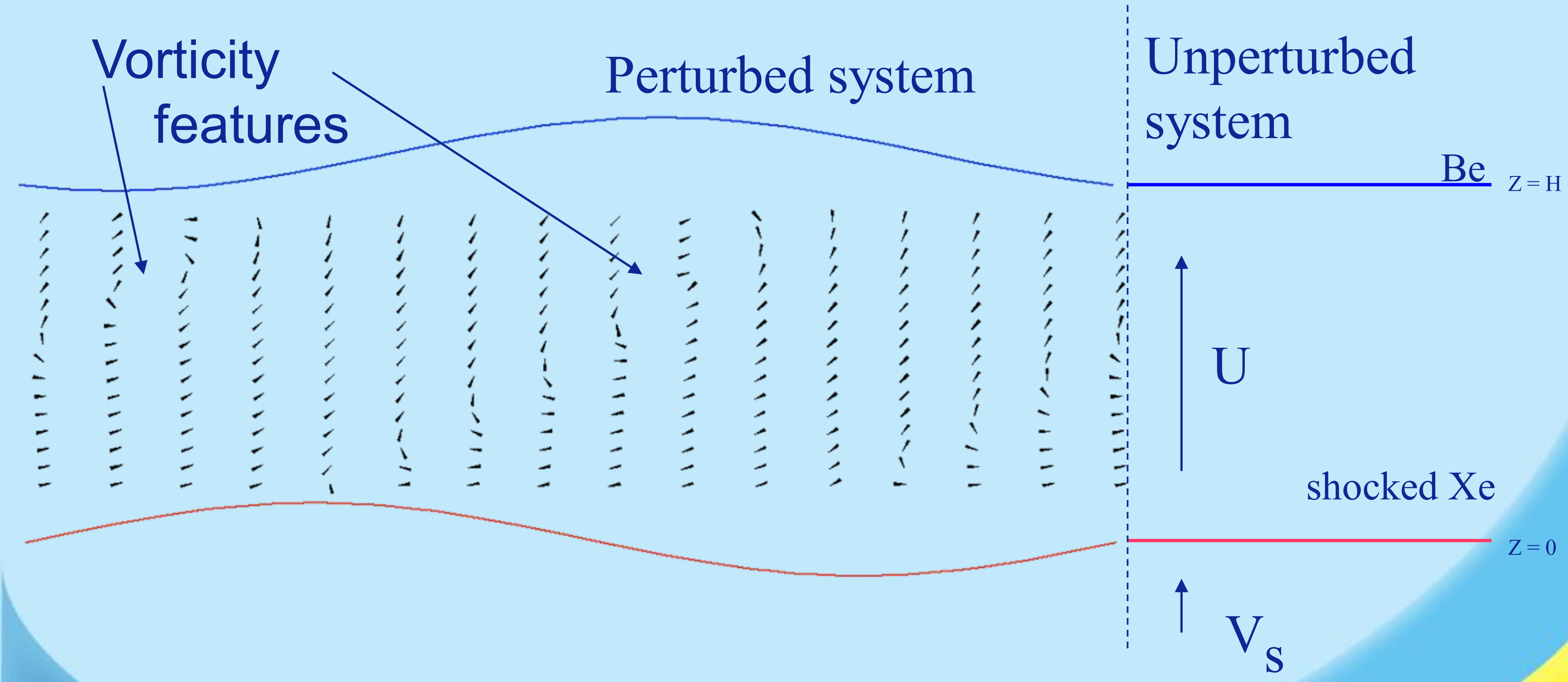

This research was supported by the DOE NNSA/ASC under the Predictive Science Academic Alliance Program by grant number DEFC52-08NA28616.

Analysis yields a dispersion relation

$$2n^4 + n^2\left(k^2 c_s^2 - \frac{\dot{V}_s^2}{c_s^2} S\right) - k^2 \dot{V}_s^2 S = 0$$

$$\text{where } S = 1 + \frac{j c_s^2}{\dot{V}_s \tanh jH}$$

- with *n* the growth for a given wavenumber *k*, and $j^2 = k^2 + c_s^2$.
- For k small, the tanh *jH* / *j* term becomes simply *H*, and solutions are analytically expressible. Otherwise, can solve this equation numerically.

This research was supported by the DOE NNSA/ASC under the Predictive Science Academic Alliance Program by grant number DEFC52-08NA28616.

Model predicts regions of instability

- The dispersion relation can be plotted for our shock parameters.
- Find a region of instability for wavelengths between about 190 to 1200 microns.
- Peak growth at about 350 microns, with growth rate $1.2 \cdot 10^8$ sec^{-1}.
- A number of these should be able to fit within our 575 micron tube.

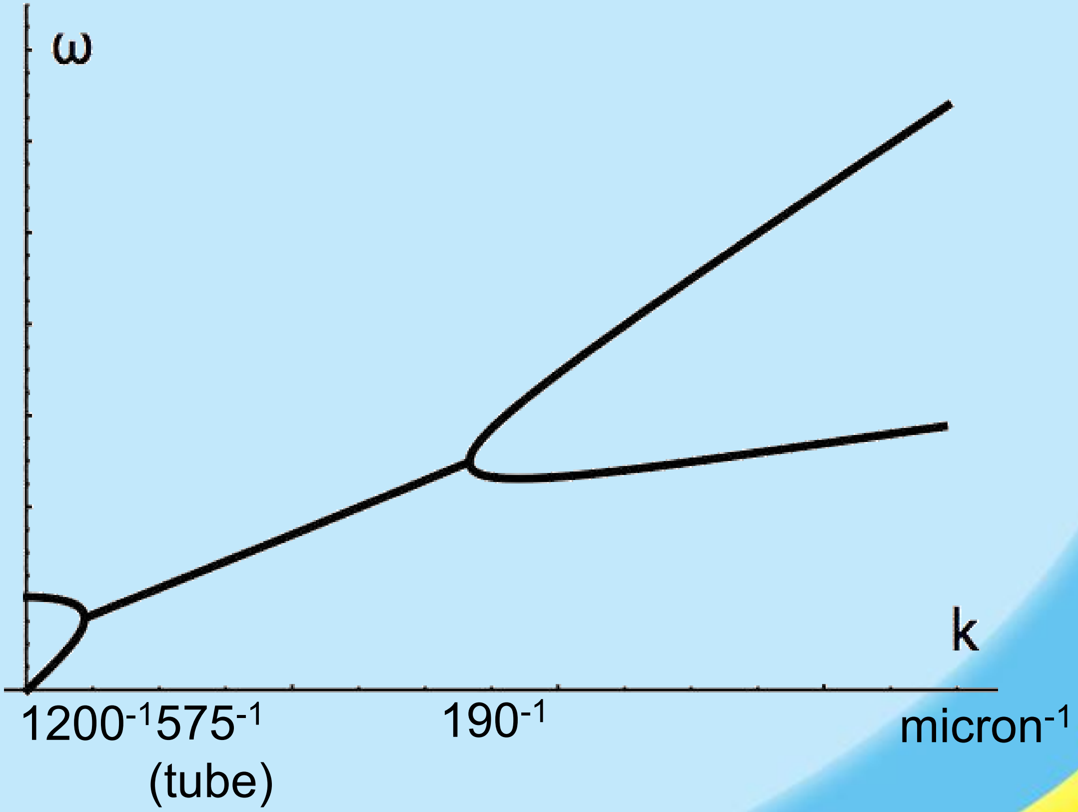

This research was supported by the DOE NNSA/ASC under the Predictive Science Academic Alliance Program by grant number DEFC52-08NA28616.

Do we have evidence of instability growth?

- Previous images may show evolution of high/low density regions

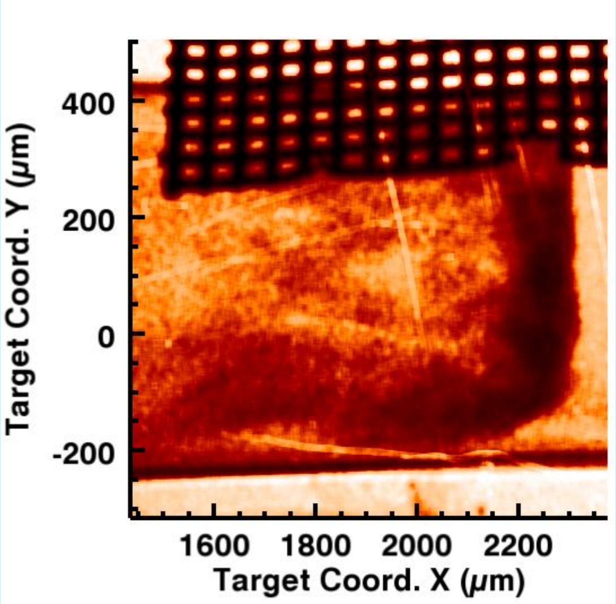

Shot 52668, 13 ns,
October 2008

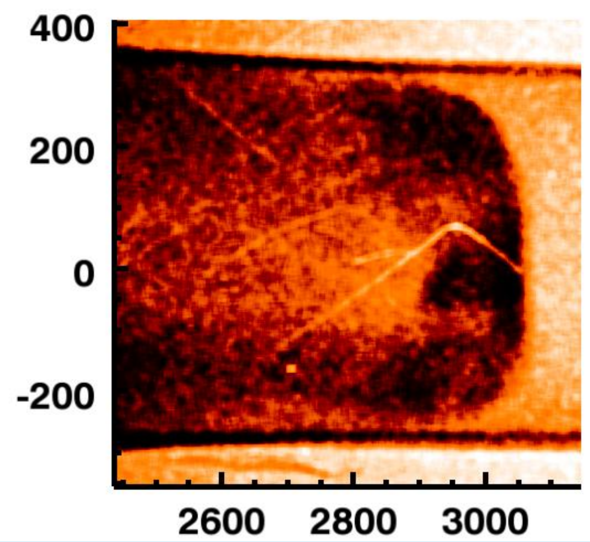

Shot 54989, 26 ns,
July 2009

This research was supported by the DOE NNSA/ASC under the Predictive Science Academic Alliance Program by grant number DEFC52-08NA28616.

Shock instability may occur in astrophysics

- This instability could be responsible for structure evolution in supernova remnants.

- Shown: SN1993J, three to five years after nova.

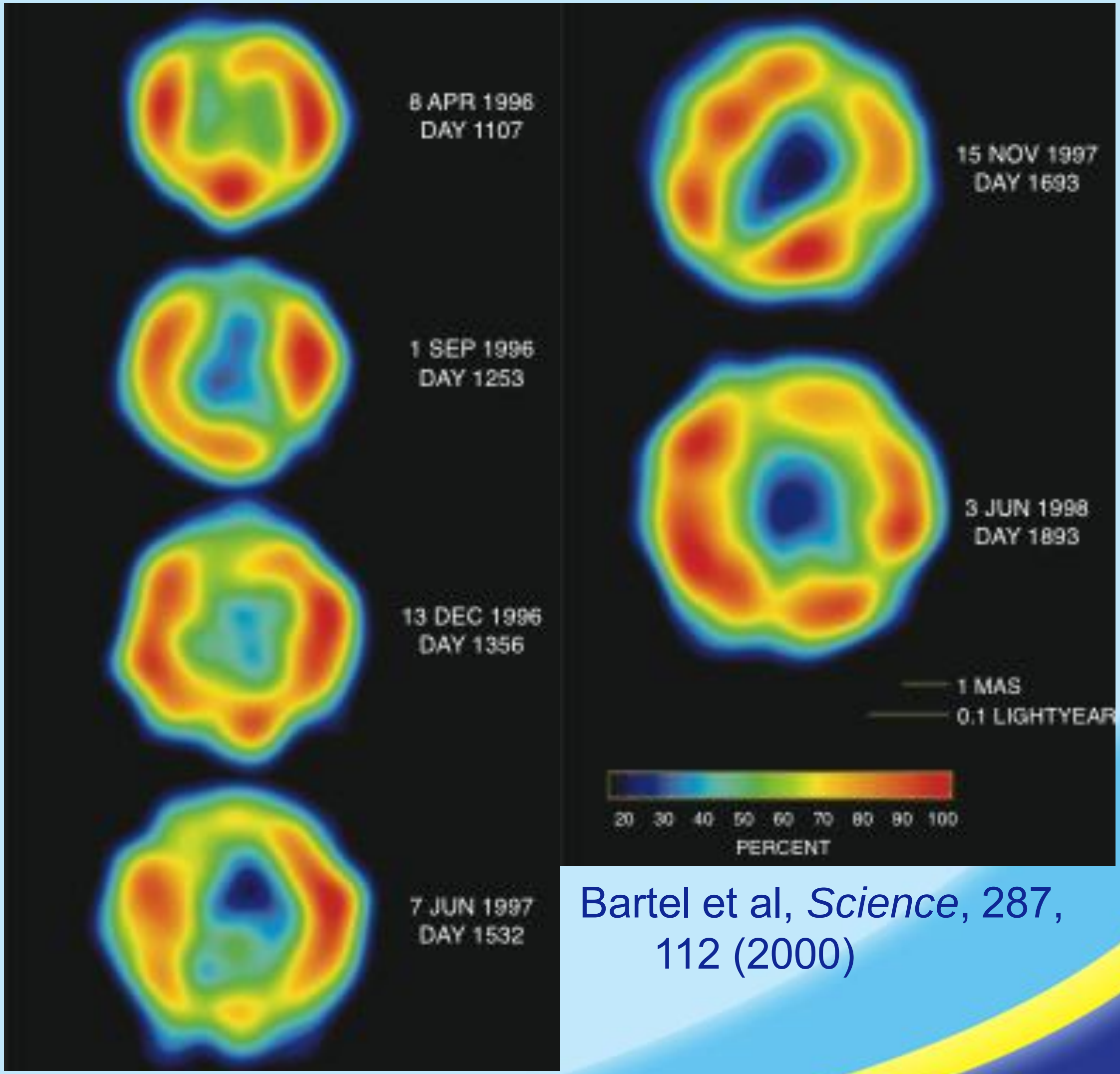

Bartel et al, *Science*, 287, 112 (2000)

This research was supported by the DOE NNSA/ASC under the Predictive Science Academic Alliance Program by grant number DEFC52-08NA28616.

The dispersion relation may be non-dimensionally scaled

$$n^4 + n^2 k^2 c_s^2 - k^2 \dot{V}_s^2 \left(1 + \frac{k c_s^2}{\dot{V}_s \tanh kH}\right) = 0$$

- The dispersion relation (here neglecting acoustic terms for simplicity) may be rewritten as a function of three dimensionless parameters.
- If two input parameters are matched in two systems, the third parameter will necessarily be equal.

$$\begin{aligned} \Pi_1 &= \frac{c_s^2}{|\dot{V}_s| H} \\ \Pi_2 &= kH \\ \Pi_3 &= \frac{c_s}{|\dot{V}_s|} n \end{aligned}$$

$$\Pi_3^4 + \Pi_1^2 \Pi_2^2 \Pi_3^2 - \Pi_1^2 \Pi_2^2 \left(1 - \frac{\Pi_1 \Pi_2}{\tanh \Pi_2}\right) = 0$$

This research was supported by the DOE NNSA/ASC under the Predictive Science Academic Alliance Program by grant number DEFC52-08NA28616.

Astrophysical and laboratory parameters are not too far off

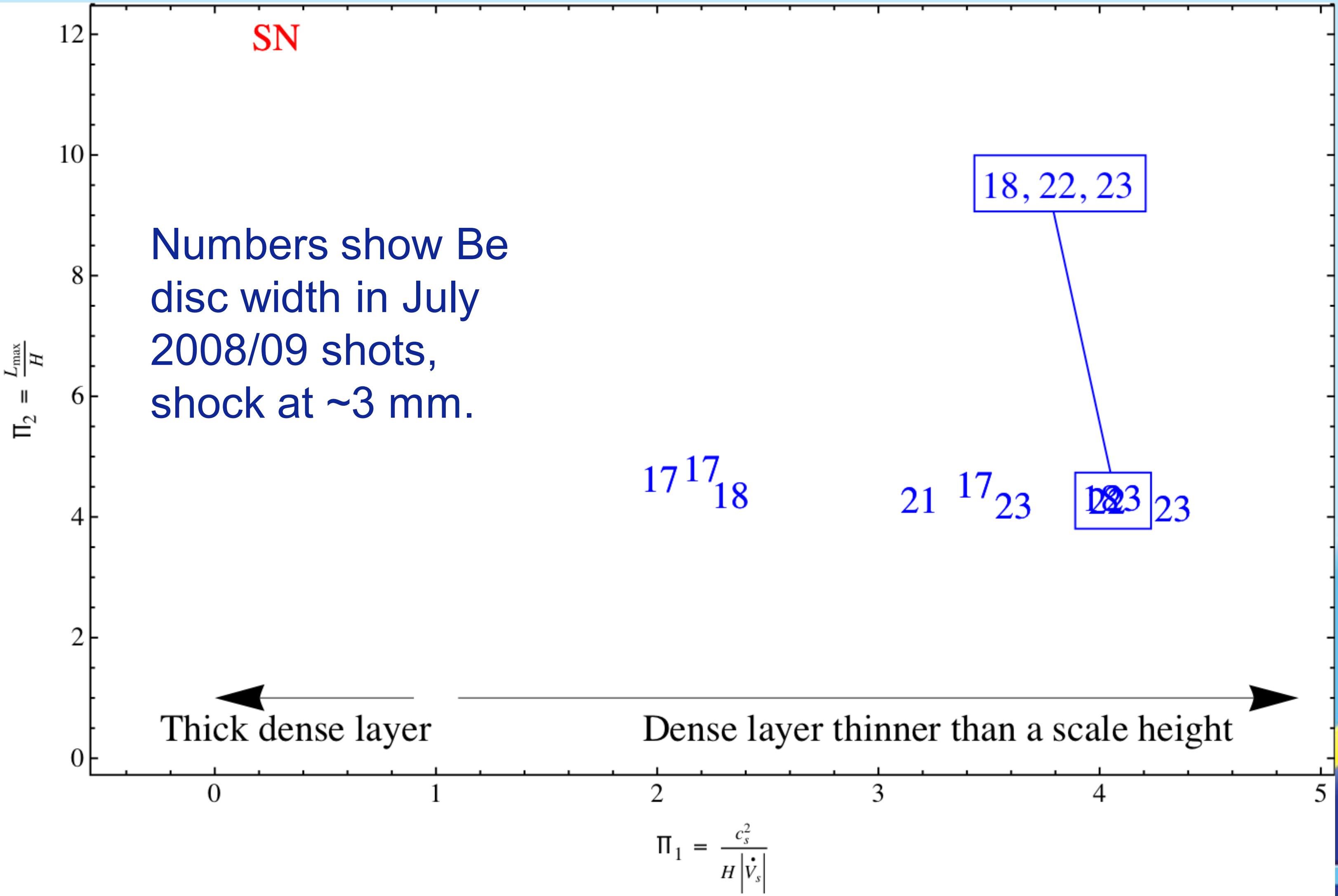

Numbers show Be disc width in July 2008/09 shots, shock at ~3 mm.

This research was supported by the DOE NNSA/ASC under the Predictive Science Academic Alliance Program by grant number DEFC52-08NA28616.